Generation of Plasma Rotation in a Tokamak by Ion-Cyclotron Absorption of Fast Alfvén Waves

F.W. Perkins,[1,2] R.B. White,[1] P.T. Bonoli,[3] V.S. Chan[2]

[1]Plasma Physics Laboratory, PO Box 451, Princeton, NJ 08543, USA
[2]General Atomics, PO Box 85608, San Diego, CA 92186-5608, USA
[3]Plasma Science and Fusion Center, MIT, Cambridge, MA 02139-4307, USA

e-mail contact of main author: perkins@fusion.gat.com

Abstract. A mechanism is proposed and evaluated for driving rotation in tokamak plasmas by minority ion-cyclotron heating, even though this process introduces negligible angular momentum. The mechanism has two elements: First, angular momentum transport is governed by a diffusion equation with a non-slip boundary condition at the separatrix. Second, Monte-Carlo calculations show that energized particles will provide a torque density source which has a zero volume integral but separated positive and negative regions. With such a source, a solution of the diffusion equation predicts the on-axis rotation frequency Ω to be $\Omega = (4q_{max}W J^{*}) eBR^3a^2n_e(2\pi)^2)^{-1}(\tau_M/\tau_E)$ where $|J^{*}| \approx 5\text{-}10$ is a nondimensional rotation frequency calculated by the Monte-Carlo ORBIT code. Overall, agreement with experiment is good, when the resonance is on the low-field-side of the magnetic axis. The rotation becomes more counter-current and reverses sign on the high field side for a no-slip boundary. The velocity shear layer position is controllable and of sufficient magnitude to affect microinstabilities.

1. Introduction

Control of plasma rotation is an effective method for optimizing magnetic fusion plasmas. Differential rotation increases the stability of fine scale modes, which cause turbulent transport, as well as of large-scale distortions of the entire plasma. In the case of turbulent modes, differential rotation breaks up their structure and prevents growth [1,2]. Large-scale modes acquire increased stability when, by differential rotation, magnetic distortions which are fixed in the frame of the plasma appear as time-dependent fluctuations in the frame of a conducting shell which surrounds the plasma. Consequently, with sufficient differential rotation, these fluctuations can not penetrate the shell, increasing the maximum pressure that can be stably confined [3,4].

The physics of plasma rotation and the generation and transport of angular momentum density is therefore interesting both as a fundamental physics process and as the basis for a plasma control tool. Review articles by Ida [5] and Chan [6] give a comprehensive account of radial electric field and plasma rotation observations and a detailed discussion of the interaction of radiofrequency heating methods with plasma rotation, respectively. Rotational response of plasmas to angular momentum input is observed to have a momentum confinement time τ_M comparable to the observed energy confinement time τ_E (cf., Section 4.2 of [5] and [7-9]) and an angular momentum diffusivity profile similar to the anomalous heat diffusivity profile.

Recently, observations of Alcator C-Mod plasmas have discovered that plasma heating by the fast-wave, minority-ion-cyclotron process can cause an appreciable co-current toroidal rotation to develop in the vicinity of the magnetic axis, even though the heating method provides negligible angular momentum [10-12]. Alcator C-Mod observations have further established that the central rotation velocity increases roughly linearly with the plasma energy content and that the rotation is strongly peaked toward the plasma center when the ion-cyclotron resonance is close to the magnetic axis. The rotation profile broadens as the cyclotron resonant surface moves to larger minor radius. The sense of rotation is co-current when the ion-cyclotron resonance lies on the low-field-side of the magnetic axis. The co-current rotation reported in ohmically-heated Alcator C-Mod plasmas [13] lies outside the scope of this work but could possibly be understood in terms of a modification of the no-slip boundary condition introduced below.

How can a plasma develop an angular momentum content when none is supplied? This paper proposes and evaluates a mechanism which resolves the apparent conflict. The argument has two parts. First, it is assumed that angular momentum transport is governed by a diffusion equation that has a no-slip boundary condition at the separatrix and a torque density source term as discussed below. If the torque-density source term has two separated regions, one with positive and the other with negative torque density, but is constrained to have zero volume-integrated torque, then the solution of the angular momentum diffusion equation will yield a finite central rotation rate. The physics picture is that angular momentum generated in the outer part of the plasma diffuses to the surface and is lost faster than that supplied to the inner part.

The second part of the argument rests on an evaluation of the torque density applied to the bulk plasma arising from the slowing down of ions accelerated by the minority-ion-cyclotron process. The cyclotron acceleration process itself introduces no angular momentum. The motivating physics picture is that, as a result of finite banana widths and collisions, a fast ion which is born on an initial magnetic surface will slow down and return to the bulk plasma over a distribution of magnetic surfaces. This constitutes a radial current in the fast particles. A neutralizing radial current then flows in the bulk plasma which produces a $j_r B_\theta R$ torque density. This is just the separated region of torque density needed to drive rotation. However this simple picture must be augmented by collisional transfer of mechanical angular momentum from the fast particles to the bulk plasma, which is of the same magnitude as the $j_r B_\theta R$ torque density. Thus a precise calculation of all sources of torque density that rigorously accounts for angular momentum is required to determine whether torque density will be applied to the bulk plasma and to determine its sense. The Monte-Carlo code ORBIT [14,15] has been modified to rigorously account for collisional momentum exchange between energetic particles and a bulk plasma as well as providing for stochastic energization by perpendicular energy diffusion. The present work differs from previous theoretical models [16] in its rigorous accounting of angular momentum, the role of radial currents associated with energetic-ion banana diffusion, and the use of a diffusive transport equation to describe plasma response to torques.

The manuscript first describes our models for fast wave propagation and ion-cyclotron heating. Next, we develop a solution to the angular momentum diffusion equation in general axisymmetric geometry defining the integrated collisional and $j_r B_\theta R$ torque densities that the ORBIT code must compute. Additions to ORBIT for this work are summarized. Results give plasma rotation curves parametrized by location of the ion-cyclotron resonance. A discussion of their sensivity to input parameters, correspondence to experiment, and a conclusion follow.

2. Two-Component Plasma Model

The starting point for our model is to separate the plasma into two components: a high-energy tail created by minority ion-cyclotron heating whose evolution will be followed by the Monte-Carlo ORBIT code and a bulk plasma, which responds to applied torque density via a diffusive angular momentum transport equation with a model momentum diffusivity profile $\chi_M = a^2 q^n / C_n \tau_M$ that spatially depends on q. Here τ_M denotes the momentum confinement time, which is taken comparable to the energy confinement time τ_E [5,9]. The motivating physics comes from the observation that if one interprets the almost linear dependence of tokamak energy confinement time on a q-dependent diffusivity, then $n \geq 2$. We will focus on $n=2$ and for which $C_2 = 2(1+\kappa^{-2})\, q_{max}$ based on an analytic power balance model.

3. Fast Wave Propagation

An important aspect of fast wave heating is that refraction focuses the waves onto the magnetic axis region and continues to maintain high wave intensities near the midplane for major radius values less than the magnetic axis. Calculations by the TORIC code [17] , portrayed in Fig. 1 illustrate this. Qualitatively, one can capture this aspect of fast wave heating by defining an intense wave region as portrayed in Fig. 1. Particles will undergo ion-cyclotron energization only if their orbits cross the cyclotron resonance surface within the

intense wave region. This has the consequence of limiting the range of magnetic surfaces where ion-cyclotron heating can take place and generating regions of high rotational shear, especially when the cyclotron resonance lies to the high-field-side of the magnetic axis. The boundary $\pm z_o$ of the intense field region has been taken to be

$$z_o = \begin{cases} z_{max} & R - R_a < z_{max} \\ R - R_a & R - R_a > z_{max} \end{cases} \qquad (1)$$

with R_a the magnetic axis major radius and z_{max} = 7 cm for Alcator C-Mod example of Fig. 1.

4. Ion-Cyclotron Heating

Two models for ion-cyclotron heating have been used. Model 1 instantaneously energizes a particle from the bulk plasma to a specified energy E_o. This initial creation is rigorously constrained to introduce zero net angular momentum and canonical angular momentum for each particle, as is appropriate for ion-cyclotron heating, and is effected by starting energetic particles with their banana tips lying on the cyclotron surface within the intense wave region. A distribution with off-midplane, banana-tip height with z, $dN/dz = \left(1-(z/z_o)^2\right)\left(2z_o - z^2\right)^{-1/2}$ is used so that only particles in the intense wave illustrated in Fig. 1 are created. The energetic ions are then followed until they lose all their energy by the Monte-Carlo ORBIT code [14,15], which includes ion-ion pitch-angle-scattering collisions [18] as well as ion and electron energy drag collisions . These collisions return energetic particles to the bulk plasma distributed over a region comparable to the banana full width about the originating magnetic surface. Our assumption that the fast waves transfer no net angular momentum to the energetic particles is rigorous for fast-waves with $k_{||} = n/R = 0$. For realistic values $n \approx \pm 10$, it can be shown that angular momentum input remains negligible for a balanced n-spectrum.

Ion-cyclotron Model 2 introduces ion-cyclotron heating by giving a particle a stochastic kick in perpendicular energy $\Delta E_\perp$ each time it passes through the cyclotron resonance surface. The kicks are given by

$$<(\Delta E_\perp)^2> = 2\, E_\perp\, E_s \qquad <\Delta E_\perp> = E_s \qquad (2)$$

where

$$E_s = c_\perp \frac{4\pi\, \nu_o q\, R_c\, E_o\, M_p^{1/2}}{\left[2(E - E_\perp) + T\right]^{1/2}} \frac{F(z)\, \alpha_c}{\left(\alpha^2 + \alpha_c^{\,2}\right)^{1/2}} \qquad (3)$$

We note that equal changes in E and $E_\perp$ leave $v_{||}$ and the canonical angular momentum unchanged. Therefore this operator introduces no angular momentum. The quantity E_s is constructed to have properties expected of ion-cyclotron heating. In particular, the mean square energy kick should be proportional to $E_\perp$, inversely proportional to $\mathbf{v}_{||}\cdot\mathbf{R}/R$, be limited to the strong wave region, and have the rate of energy increase for a particle injected at energy E_o comparable to its loss of energy via coulomb collisions. Thus, E_s, as given below, is a function of R_c, z, ν_o, E, $E_\perp$,q, E_o, and T — all evaluated at the cyclotron resonance crossing point. The adjustable constant $c_\perp$ governs the energy input via ICRF heating to be large, but not very large, compared to the initial particle parameter $\nu_o E_o$. It is expected that $c_\perp$ will be close to unity. The parameter $\alpha = \alpha(R_c, z) = \mathbf{R}\cdot\phi\times\nabla\psi(R\,\nabla\psi)^{-1}$ depends only on magnetic surface geometry and reflects the degree of tangency between the magnetic surface and the cyclotron resonant surface. An ad-hoc cutoff at $\alpha_c = 0.1$ prevents mathematical divergences. The formula for F(z) describes the strong field region

$$F(z) = \sqrt{2}\left(1 - \frac{z^2}{z_o^{\,2}}\right)\left(2 - \frac{z^2}{z_o^{\,2}}\right)^{-1/2} \qquad (4)$$

With this model, initial particle parameters are a monoenergetic, isotropic velocity distribution at energy E_o and are distributed uniformly in space for $\Phi(R_c,0) < \Phi < \Phi(R_c, z_o)$.

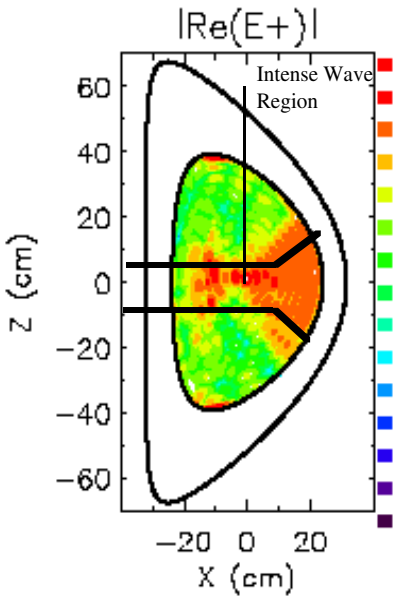

FIG. 1. Propagation of the fast wave in Alcator C-Mod when the ion-cyclotron resonance lies at -8 cm, well to the high-field-side of the magnetic axis. The toroidal mode number is n=10 is representative of the antenna spectrum.

This initial condition introduces zero angular momentum. Again, particles are followed by ORBIT until they reach zero energy. This model is closer to actual ion-cyclotron heating, but produces a bias rotation, which we discuss and correct for below.

5. Angular Momentum Diffusion

The general, steady-state axisymmetric angular momentum transport equation equates angular momentum flux through a flux surface to the torque generated inside that surface.

$$\oint \mathbf{dl} \times \phi \cdot \hat{\nabla}\Phi \, 2\pi R^3 \, n M (\chi_o q^n) \frac{\partial \Omega}{\partial \Phi} = -\, T(\Phi) \dot{N} R_a^2 \Omega_a \qquad (5)$$

where Φ denotes the area enclosed by a magnetic surface in the poloidal plane and serves as the independent flux-surface label. Here Ω denotes the angular rotation rate, which must be constant on a flux surface, and $T(\Phi)$ is the nondimensional integrated torque-per-particle exerted on the plasma inside magnetic surface Φ and is computed by ORBIT. The fundamental mass, length, and frequency units used by ORBIT are the proton mass, the major radius, and the ion-cyclotron frequency, both evaluated at the magnetic axis. $\dot{N}$ denotes the rate at which particles are supplied and is related to the applied power through $\dot{N} E = P$ where E is the average net energy-per-particle transferred from the energetic particles to the bulk plasma. For ion cyclotron Model 1, $E=E_o$.

We will neglect variations of R and the effective diffusivity $\chi_o q^n$ on a magnetic surface. Equation (5) can then be recast as

$$\frac{1}{\dot{N}} \frac{\partial \Omega}{\partial \Phi} = -\frac{T(\Phi)\, \Omega_a}{8\pi^2 \, \Phi \, H(\Phi) \, n \, R \left(\chi_o q^n\right)} \qquad (6)$$

where $H(\Phi)$ is defined by

$$4\pi \, \Phi \, H(\Phi) = \oint \mathbf{dl} \times \boldsymbol{\phi} \cdot \hat{\nabla} \, \Phi = \int dA \;\; \nabla^2 \Phi \qquad (7)$$

where the integral is over the area inside the magnetic surface. It can be shown that $H(\Phi)$ is a surface function, will be close to unity, and depend only weakly on the shape of the magnetic surface. Therefore, the expression for the rotation rate becomes

$$\frac{1}{\dot{N}} \left(\Omega(\Phi) - \Omega(\Phi_{max}) \right) = \left(\frac{\Omega_a}{8\pi^2 \, n \, R \, \chi_o} \right) \int_{\Phi}^{\Phi_{max}} \frac{T(\Phi) \, d\Phi}{\Phi \, q^n} \quad . \qquad (8)$$

The integrated torque will also have a surface contribution when particles are being lost from the plasma. The requirement for zero angular momentum input is $T(\Phi_{max}) = 0$. Equation (8) computes the rotation rate from the Integrated Torque T. Angular momentum conservation requires $T(\Phi_{max}) = 0$. A simple q-profile is employed $q = 1+(q_{max}-1)\cdot(\Phi/\Phi_{max})$.

The physics rationale for a surface no-slip boundary condition $\Omega(\Phi_{max}) = 0$ derives from the property of ideal MHD that axisymmetric equilibria must have Ω a function of flux-surface only combined with the observation that the separatrix flux surface is line-tied to a fixed conducting material boundary and so can not rotate. In reality, the complex and strong radial

electric fields found in the H-mode pedestal may well alter the boundary condition from that of simple ideal MHD considerations[19]. Observation of rotation in Ohmic H-modes are consistent with this picture.

Since the principal contribution to the integral for Ω is expected to come from a thin layer whose thickness scales with the gyroradius, this integral will be rescaled by a factor v^{-1}, where $v = (2E/M)^{1/2}(R_a\omega_{ci})^{-1}$. We also introduce T^* via $T = \dot{N}T^*v$, where $\dot{N}$ is the rate at which is the rate at which the plasma heating is supplying energetic particles of energy E so the fast-wave heating power $P = \dot{N}E$. T^* has the interpretation of being the angular momentum transferred from an average energetic particle to the bulk plasma inside flux surface Φ in units of $(2EM)^{1/2}R_a$. Thus, the expression for the rotation rate becomes

$$\frac{\Omega(\Phi) - \Omega(\Phi_{max})}{\dot{N}} = \frac{v^2}{2(2\pi)^2\langle n\chi_o\rangle} I_n^*(\Phi) \qquad I_n^*(\Phi) = \frac{1}{V}\int_{\Phi}^{\Phi_{max}} \frac{d\Phi'}{\Phi' q^n} T^*(\Phi') \qquad (9)$$

Numerical results reported below will confirm that, with this scaling, I^* is insensitive to particle energy.

6. ORBIT Calculations of Integrated Torque

Equation (9) reduces our problem to the calculation angular momentum driven in the bulk plasma by the ensemble average of individual particles. The complex evolution of particle orbits, with pitch angle scattering transforming orbits from trapped to passing and back again, suggests the use of a Monte-Carlo method. The ORBIT code [14,15], which follows particle banana and passing orbits and their evolution by collisions [18], while strictly conserving angular momentum, has been adapted to this problem.

The ORBIT code follows an ensemble of Monte-Carlo particles with the initial condition as specified in the preceding paragraph as their orbits evolve under the influence of collisions. The collision model is ion-ion pitch angle scattering and energy drag of minority ions against a cold bulk deuterium plasma and electrons, as given by

$$\frac{1}{E}\left(\frac{dE}{dt}\right) = -2\nu_o\left(\frac{E_o}{E}\right)^{3/2}\left\{\frac{M_p}{M_d} + \frac{4}{3\sqrt{\pi}}\left(\frac{m_e}{M_p}\right)^{1/2}\frac{E^{3/2}}{T^{3/2}}\right\} \qquad d\langle\theta^2\rangle/dt = \nu_o\left(E_o/E\right)^{3/2} \qquad (10)$$

where $\nu_o = 2\pi\sqrt{2}\,n_e e^4 \ell n\Lambda\, M_p^{-1/2}E_o^{-3/2}$ and E_o is the initial particle energy.

ORBIT records the angular momentum increment $MR(\Delta v_{||})$ [in units of $(2ME)^{1/2}R_a$] received by a Monte-Carlo particle in each collision event as well as the magnetic surface on which the collision took place. An equal but opposite angular momentum increment is then accumulated in one of the 10,000 computational bins in toroidal flux corresponding to the magnetic surface where the collision occurred. From this data one forms $T_2^* \int_0^{\Phi} MR\Delta v_{||} d\Phi$, which is the Monte-Carlo ensemble average angular momentum impulse imparted to the bulk plasma within flux surface Φ by collisions with energetic particles.

Torque also arises from the radial currents which result when a particle comes to rest on a magnetic surface which differs from their originating one. It is straight forward to show that the total torque δT exerted on a shell of thickness $\delta\psi$ in poloidal flux is given by the radial current I_r. The radial current is determined in turn by the fraction of particles which come to rest inside a given magnetic surface. For each Monte Carlo particle, the ORBIT code records the initial magnetic flux surface Φ_o and its final position is assigned to one of the bins. From this data one can form

$$T_1^* = \frac{1}{V}\int_0^{\Phi} \frac{d\Phi'}{q} G(\Phi') \qquad G(\Phi) = \begin{cases} F(\Phi) & \Phi < \Phi_o \\ 1 - F(\Phi) & \Phi > \Phi_o \end{cases} \qquad (11)$$

and $F(\Phi)$ is the average number of particles whose final position is inside surface Φ. T_1^* is the angular momentum given to the bulk plasma by a single ensemble-average particle

through Rj_rB_θ torques [in units of $(2ME)^{1/2}R_a$] . The discontinuity in $G(\Phi)$ arises from subtraction of a cold bulk particle in the initial conditions.

Lastly, when particles are lost from the plasma, they carry with them their mechanical angular momentum which is accumulated as T_3^*. At the plasma surface the total integrated torque $T_1^* + T_2^* T_3^*$ is evaluated and found to vanish with a relative accuracy of $2 \cdot 10^{-3}$ or better. Thus, our physics and computational scheme does not introduce any angular momentum.

This completes our formalism. Monte Carlo runs determine $F(\Phi)$, $T_1^*(\Phi)$, $T_2^*(\Phi)$, and finally $I^*(\Phi)$. Because our final expression involves two integrations over the distributions in computational bins, the results are very insensitive to the number of bins and adequate accuracy results from 1000 Monte Carlo particles per run.

7. Results

Non-dimensional rotation integrals I_2^* for a scan of resonance surface locations are presented for a circular tokamak model for Alcator C-Mod, based on ion-cyclotron Model 1 which starts particles at an energy of 48 keV with their banana tips on the cyclotron resonance surface in the intense wave region. The magnetic axis lies at $R_c =$ 67 cm and $q_{max} = 4.0$. Calculations done with an initial energy of 24 keV and with different initial pitch confirmed insensitivity to input parameters except resonance location. Fig. 2 displays the results. One notes the following features: The magnitude of the central rotation is $|I_2^*| = 5\text{-}10$. The rotation profiles are small outside the cyclotron resonance surface (except for R=51 which had appreciable lost particles). And, the sense of rotation changes from co-current to counter-current as the resonance surface passes through the magnetic axis.

Ion cyclotron Model 2, with perpendicular energy diffusion, has a potential for bias arising from its initial conditions. This arises from the results of calculations in which starting energetic particles in pairs of equal but opposite parallel velocity resulted in driving a rotation. Although contributions from a range of major radius values produce an approximate cancellation, a residual rotation remains. Consequently, we compute the difference between rotation profiles of a reference case without ICRF heating and a case with the same initial conditions, but with ICRF. We then form

$$J_2^* = \frac{E_o}{E_{ICRF} - E_o}\left(I_{2\,ICRF}^* - I_{2\,Ref}^*\right) \qquad (12)$$

which gives the incremental rotation normalized by the incremental energy, which is the difference between the starting energy and the total average energy transferred by a particle to the bulk plasma. Fig. 3 presents results for an initial energy of 10 keV and $c_\perp = 1.0$, which resulted in a modest increase of particle energy due to ICRF heating. It is evident that these two models produce effectively equivalent rotation profiles.

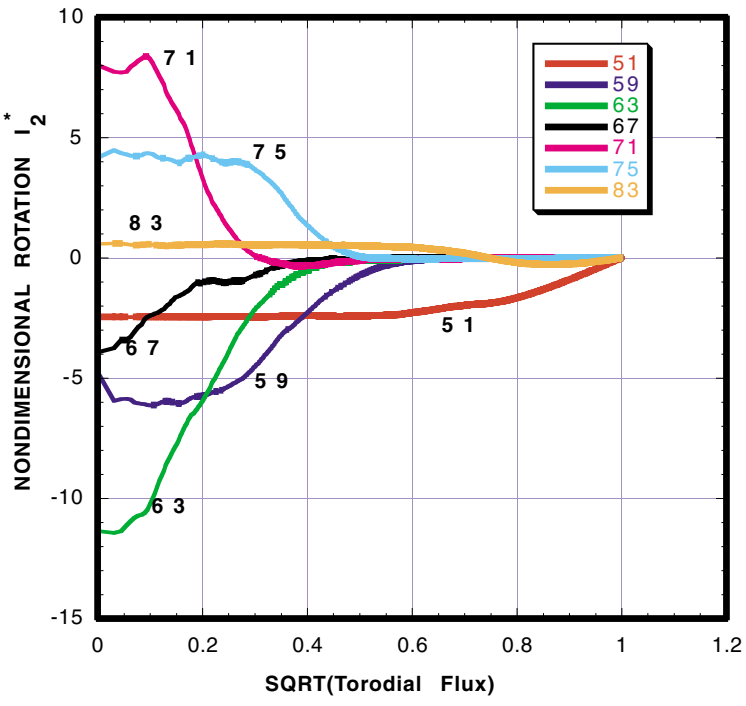

FIG. 2. Nondimensional rotation profiles I_2^* for ICRF model 1.1 versus square root of normalized toroidal flux for various values of the major radius of cyclotron resonance surface. Magnetic axis is R = 67 cm.

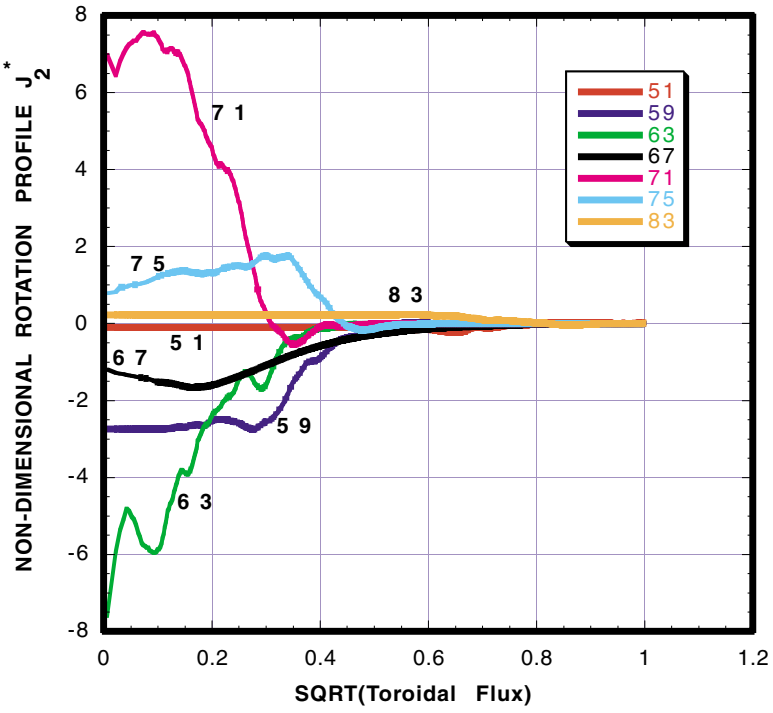

FIG. 3. Nondimensional Rotation profiles J_2^* for ion-cyclotron model 2 with the major radius of cyclotron resonance layer as a parameter.

Figure 4 presents the integrated torque profiles T_1^* and T_2^* for R=71 cm. It is evident that the co-current torque by collisional mechanical angular momentum transfer is what generates the co-current rotation. This plot attests to the accuracy of the ORBIT code in attaining zero integrated torque at the plasma boundary.

Putting the results into dimensional form, the rotational profile takes the form

$$\Omega - \Omega_{boundary} = \frac{4 q_{max} W}{eBR^3 a^2 n_e (2\pi)^2} \left(\frac{\tau_M}{\tau_E} \right) I_2^* \qquad (13)$$

where W denotes plasma energy content. Based on $I_2^* \approx 8$ and $n_e = 3 \cdot 10^{20} m^{-3}$, Eq. (13) gives a central rotation rate of 110 krad/s, the observed rate in Alcator C-Mod, for the no-slip boundary condition $\Omega_{boundary} = 0$.

Lets us also note that off-axis resonance locations (cf., R=59 cm and 75 cm) produce layers of high velocity shear that are strongly localized. The velocity shear values are roughly $8 \cdot 10^5$Hz for C-Mod parameters, are comparable to drift wave frequencies (less than 10^6 Hz), and therefore should be effective at stabilizing drift waves and producing internal transport barriers.

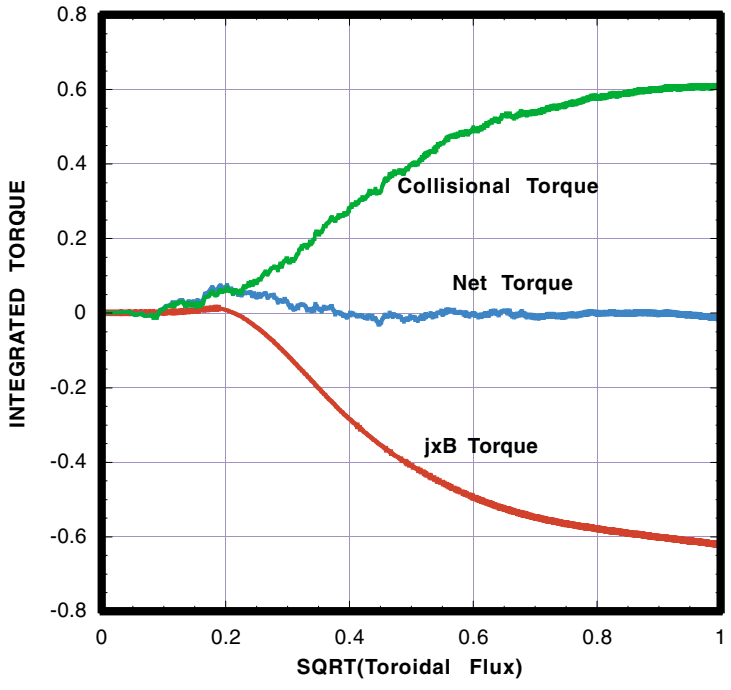

FIG. 4. Integrated torque for ICRF model 1.1 at R= 71 cm.

8. Conclusion

Overall, we can conclude that a physics basis exists for ICRF heating to be an effective free energy source which creates torque densities that can generate rotation and velocity shear, when coupled with diffusive transport of angular momentum. Quantitative agreement is obtained between theory and experiment. A key prediction is the changing the sense of plasma rotation depending on the location of

cyclotron resonance surface. The surface boundary condition remains a source of uncertainty. We have benefited from discussions with J. Rice, M. Porkolab, and Y. Omelchenko. This work was supported by US DOE Contracts DE-AC02-76CH03073. DE-AC03-99ER54463, and DE-FG02-90ER54084.

References

[1] BURRELL, K.H., Phys. Plasmas **4** (1997) 1499.
[2] WALTZ, R.E., et al., Phys. Plasmas **5** (1998) 1784.
[3] CHU, M.S., et al., Phys. Plasmas **2** (1995) 2236.
[4] TAYLOR, T.S., et al., Phys. Plasmas **2** (1995) 2390.
[5] IDA, K., Plasma Phys. Control. Fusion **40** (1998) 1429.
[6] CHAN, V., et al., in Radio Frequency Power in Plasmas (1999, American Instate of Physics) 45.
[7] HAWRYLUK, R.J., et al., Plasma Phys. Control. Fusion **33** (1991) 1509.
[8] BURRELL, K.H., et. al., Nuclear Fusion **28** (1988) 3.
[9] SCOTT, S.D., et al., Phys. Rev. Lett. **64** (1990) 531.
[10] RICE, J.E., et al., Nuclear Fusion **38** (1998) 75.
[11] RICE, J.E., et al., Nuclear Fusion **39** (1999) 1175.
[12] RICE, J.E., et al., Phys. Plasmas **7** (2000) 1825.
[13] HUTCHINSON, I.H., et al., Phys. Rev. Lett. **84** (2000) 3330.
[14] WHITE, R.B., Phys. Fluids B **2** (1990) 845.
[15] WHITE, R.B. , CHANCE, M.S., Phys. Fluids **27** (1984) 2455.
[16] CHANG, C.S., et al., Phys. Plasmas **6** (1999) 1969.
[17] BRAMBILLA, M., Nuclear Fusion **38** (1998) 1805.
[18] BOOZER, A.H. , KUO_PETRAVIC, G., Phys. Fluids **25** (1981) 851.
[19] BURRELL, K.H., Phys. Plasmas **6** (1999) 4418.